Microscale Collagen and Fibroblast Interactions Enhance Primary Human Hepatocyte Functions in Three-Dimensional Models

David A. Kukla,* Alexandra L. Crampton,† David K. Wood,† and Salman R. Khetani*

*Department of Bioengineering, University of Illinois at Chicago, Chicago, IL, USA
†Department of Biomedical Engineering, University of Minnesota, Minneapolis, MN, USA

Human liver models that are three-dimensional (3D) in architecture are indispensable for compound metabolism/toxicity screening, to model liver diseases for drug discovery, and for cell-based therapies; however, further development of such models is needed to maintain high levels of primary human hepatocyte (PHH) functions for weeks to months. Therefore, here we determined how microscale 3D collagen I presentation and fibroblast interaction affect the longevity of PHHs. High-throughput droplet microfluidics was utilized to generate reproducibly sized (~300-μm diameter) microtissues containing PHHs encapsulated in collagen I ± supportive fibroblasts, namely, 3T3-J2 murine embryonic fibroblasts or primary human hepatic stellate cells (HSCs); self-assembled spheroids and bulk collagen gels (macrogels) containing PHHs served as controls. Hepatic functions and gene expression were subsequently measured for up to 6 weeks. We found that microtissues placed within multiwell plates rescued PHH functions at 2- to 30-fold higher levels than spheroids or macrogels. Further coating of PHH microtissues with 3T3-J2s led to higher hepatic functions than when the two cell types were either coencapsulated together or when HSCs were used for the coating instead. Importantly, the 3T3-J2-coated PHH microtissues displayed 6+ weeks of relatively stable hepatic gene expression and function at levels similar to freshly thawed PHHs. Lastly, microtissues responded in a clinically relevant manner to drug-mediated cytochrome P450 induction or hepatotoxicity. In conclusion, fibroblast-coated collagen microtissues containing PHHs display high hepatic functions for 6+ weeks and are useful for assessing drug-mediated CYP induction and hepatotoxicity. Ultimately, microtissues may find utility for modeling liver diseases and as building blocks for cell-based therapies.

Key words: Droplet microfluidics; Spheroids; 3T3-J2; Hepatic stellate cells (HSCs)

INTRODUCTION

Owing to significant species-specific differences in drug metabolism functions, in vitro models of the human liver are now utilized during preclinical development to assess human-relevant metabolism and toxicity of pharmaceuticals and industrial chemicals[1]. Such models are also being applied to mimic key cell phenotypes in liver diseases to enable novel drug discovery and to explore the potential of cell-based therapies for patients suffering from end-stage liver disease[2,3]. Human liver models can be constructed using transformed cell lines and induced pluripotent stem cell-derived human hepatocytes; however, drug metabolism capacities of both cell sources remain very low[4]. Additionally, precision cut liver slices lose viability within days due to inflammation[1]. Therefore, isolated primary human hepatocytes (PHHs) are typically the cell type of choice for building human liver models[5], and novel strategies are being devised to harness in vivo-like replicative potential of PHHs toward increasing supply for downstream applications[6].

In contrast to rapidly dedifferentiating PHHs cultured onto collagen I adsorbed onto plastic dishes[7], several advanced two-dimensional (2D) and three-dimensional (3D) culture platforms have been developed to prolong PHH functional lifetime to 2–4 weeks in vitro; hepatic functions are typically enhanced in such platforms upon coculture with liver- or non-liver-derived nonparenchymal cell (NPC) types[1]. For instance, when housed in micropatterned cocultures (MPCCs) with 3T3-J2 murine embryonic fibroblasts, PHHs display a higher level of phenotypic stability than possible with randomly distributed cocultures of the same two cell types[7]. However,

Address correspondence to Salman R. Khetani, Ph.D., Department of Bioengineering, University of Illinois at Chicago, 851 S Morgan Street, 218 SEO, Chicago, IL 60607, USA. Tel: 312-413-9424; Fax: 312-996-5921; E-mail: skhetani@uic.edu or David K. Wood, Ph.D., Department of Biomedical Engineering, University of Minnesota, 7-105 Nils Hasselmo Hall 312 Church Street SE, Minneapolis, MN 55455, USA. Tel: (612) 624-1438; E-mail: dkwood@umn.edu

the adsorbed collagen in MPCCs is insufficient to reca- pitulate the 3D cell–cell and cell–extracellular matrix (ECM) interactions in physiology and as remodeled in diseases such as fibrosis; furthermore, 2D liver models are not suitable for use as building blocks in regenera- tive medicine (i.e., cell-based therapies). Similar limita- tions are apparent in those liver-on-a-chip microfluidic devices that culture PHHs in monolayers on synthetic or natural membranes[8,9]. Furthermore, relative to static mul- tiwell plates that are amenable to industrial-scale robotic infrastructure, perfusion-based devices (i.e., liver-on- a-chip) typically reduce the throughput for drug testing and require fluid handling equipment that adds to assay cost. In contrast, 3D liver models, such as self-assembled spheroids and bioprinted liver tissues placed within static multiwell plates, can mitigate the above limitations with static or perfused 2D models. Spheroids, in particular, can be created in different types of multiwell plates for com- pound screening[10,11]. However, it is difficult to form struc- turally stable spheroids with >50% of PHH donors/lots (and, thus, spheroid-qualified PHH lots are available at a significant premium from commercial vendors), poten- tially due to variable ECM secretion rates across donor cells, while bioprinting is an expensive and low-through- put process requiring an unsustainably large number of expensive PHHs for compound screening applications[12]; therefore, further improvements in 3D human liver models are needed to mitigate the abovementioned limitations.

PHH functions are highly sensitive to the ligation of integrins to proteins within the ECM; thus, encapsulat- ing PHHs within ECM hydrogels at adequate cell densi- ties has been shown to induce liver functions in vitro[5,13]. However, large (>500 μm) ECM hydrogels that encapsu- late cells pose significant diffusion limitations for oxygen and nutrients in the construct's core in the absence of a functional vasculature[14]; this limitation can be mitigated by miniaturizing the hydrogel scaffolds to ~100–300 μm, albeit it is not trivial to create reproducible hydro- gel scaffolds of this size via manual pipetting. Thus, in recent years, investigators have employed microfluidics to produce highly monodisperse microscale emulsions (droplets) in a high-throughput format[15,16]. This so-called "droplet microfluidics" is ideally suited to precisely tune at the microscale cell–cell and cell–ECM interactions and determine optimal conditions for cell survival and func- tion. A few studies have demonstrated the use of droplet microfluidics for liver cell culture. Chen et al. encapsu- lated HepG2 cells in an aqueous droplet surrounded by an alginate shell containing NIH-3T3 fibroblasts, which pro- moted HepG2 function[17]. In contrast, Siltanen et al. devel- oped a coaxial flow-focusing droplet microfluidic device to fabricate microcapsules with a liquid core contain- ing primary rat hepatocytes and a poly(ethylene glycol) (PEG) gel shell; such a droplet configuration promoted

tight hepatocyte interactions. and further culturing the hepatocyte droplets atop a 3T3-J2 layer led to higher hepatic functions for 12 days than hepatocyte droplets alone[18]. Similarly, Li et al. first created 2D micropatterns of primary rat hepatocytes with controlled cell–cell inter- actions and then lifted such micropatterns using collage- nase followed by encapsulation into PEG-based droplets; inclusion of 3T3-J2 into the droplets led to higher hepatic function for 16 days[19]. Finally, Schepers et al. created self-assembled spheroids of PHHs and 3T3-J2, encap- sulated them into PEG-based droplets, and demonstrated human liver function for 8 days[20].

While the studies above show the high-throughput generation of liver droplets using a variety of hepatic cell sources, it remains unclear whether encapsulating PHH/ fibroblast spheroids within bioinert or adhesive peptide- functionalized PEG or alginate-based droplets can sus- tain *human* liver functions beyond a week[20]; the ability to retain PHH functions for several weeks and even months is important for modeling the chronic effects of drugs and disease stimuli as in the clinic toward devel- oping effective drug therapies for different stages of the diseases. Ultimately, the use of a natural ECM may be necessary for maintaining PHH functions long term at physiologically relevant levels in 3D models as has been shown in 2D models that routinely utilize collagen and/or Matrigel™[5]. Therefore, here we sought to adapt our pre- viously developed droplet microfluidic device useful for rapidly fabricating protein microgels[15,16] to (a) determine the optimal device and culture conditions for the creation of PHH/collagen droplets (microtissues) in multiwell plates, (b) elucidate the role of different fibroblast popu- lations [3T3-J2 and primary human hepatic stellate cells (HSCs)] on the long-term (6+ weeks) enhancement and stabilization of PHH functions when the two cell types were either coencapsulated within the collagen droplets or when the fibroblasts were "coated" on the outside of the PHH-containing collagen droplets, (c) determine the differences in hepatic functional output within microtis- sues relative to conventional self-assembled spheroids and collagen bulk hydrogels (macrogels), and, finally, (d) determine the utility of the microtissues for assays in drug development, specifically drug-mediated cyto- chrome P450 (CYP450) induction and drug-induced hepatotoxicity.

MATERIALS AND METHODS

Microfluidic and Microwell Device Fabrication

Polydimethylsiloxane (PDMS)-based microfluidic devices consisting of a single emulsion droplet generator with 300-μm straight channel and 150-μm nozzle were fabricated, bonded to glass slides, and coated with hydro- phobic Novec™ 1720 (3M, Maplewood, MN, USA) using published procedures[15]. Molten agarose (2% w/v) was

prepared and dispensed into each well of a 24-well tissue culture polystyrene plate. PDMS stamps with ~1,000 micropillars were placed into the molten agarose within each well of a 24-well polystyrene plate. After the agarose cooled, the PDMS stencils were removed, forming ~300-μm-diameter × ~300-μm-deep wells (microwells) in the casted agarose[16]. PDMS devices and agarose microwells were sterilized via autoclaving or 70% ethanol treatment (1 h), respectively.

PHH Monocultures

A solution of rat tail collagen, type I (Corning Life Sciences, Tewksbury, MA, USA), in acetic acid was first diluted in 1× phosphate-buffered saline (PBS; Corning) to 6 mg/ml on ice, and then the pH was neutralized to 7.4–7.6 using 1 N NaOH. Cryopreserved PHHs (lot HUM4055A, 54-year-old female Caucasian, and HUM4192, 16-year-old female Asian; Lonza, Walkersville, MD, USA) were thawed, counted, and viability (>85%) was assessed as previously described[21]. PHHs were resuspended in the neutral collagen solution at varying densities (1.25e6 to 5e6 cells/ml). The collagen solution containing cells was perfused into the microfluidic device inlet at 150 μl/h in a cold room (4ºC) while fluorocarbon oil (FC-40, Sigma-Aldrich, St. Louis, MO, USA) with 2% 008-fluoro-Surfactant (RAN Biotechnologies, Beverly, MA, USA) was perfused at 650 μl/h at the T-junction to produce PHH/collagen emulsions (herein referred to as "microtissues"). Microtissues were collected in a 1.5-ml tube that was heated at 37°C to promote collagen polymerization. Polymerized microtissues were rinsed, resuspended in culture medium, counted, and seeded into the agarose microwells within a 24-well plate (~600 microtissues/well). Hepatocyte culture medium, the composition of which was described previously[22], was replaced on microtissues every 4 days (400 μl/well).

Conventional 2D monocultures were created by seeding PHHs at a density of 350K cells in 400 μl/well of 24-well plates. Conventional 3D PHH monocultures were created by either seeding PHHs directly into agarose microwells (200K cells in 400 μl/well in a 24-well plate) to form self-assembled spheroids or by seeding a PHH and collagen (6 mg/ml) mixture (20K cells in 200 μl/well of collagen) directly in a 24-well plate to form bulk gels (herein referred to as "macrogels").

Cocultures of PHHs With 3T3-J2 Murine Embryonic Fibroblasts or Primary HSCs

3T3-J2 fibroblasts and primary HSCs were passaged onto tissue culture plastic as previously described[23]; the HSCs become myofibroblasts when passaged in vitro. Both fibroblast cell types were subsequently growth arrested by incubating with 1 μg/ml mitomycin-C (Sigma-Aldrich) in culture medium for 4 h prior to detachment from the

culture substrates using trypsin as previously described[7]. Microtissues were created as described above except that the PHHs and 3T3-J2 fibroblasts at a 1:1 ratio were first cosuspended in the collagen solution prior to injection into the microfluidic device to create "coencapsulated" microtissues. Alternatively, PHH-only microtissues were created, placed into agarose microwells within a 24-well plate, and then 3T3-J2 fibroblasts or HSCs were seeded onto the polymerized PHH microtissues at ~1:1 PHH/fibroblast or HSC ratio; the fibroblasts or HSCs preferentially attached to the collagen microtissues as opposed to the nonadhesive agarose to create so-called "coated" coculture microtissues. Additionally, PHH-only microtissues were created, placed into agarose microwells within a 24-well plate, and then 3T3-J2 fibroblasts were seeded into a Transwell™ insert at ~1:1 PHH/fibroblast ratio to enable paracrine-only interactions between the cell types. Culture medium was replaced as described above for PHH monocultures.

For control models, self-assembled PHH/3T3-J2 spheroids were created by seeding PHHs into agarose microwells as described above and then seeding 3T3-J2 fibroblasts the next day at a 1:1 ratio with the PHHs (200K cells/well for each cell type in a 24-well plate). Finally, PHH-containing macrogels were created as described above, and then 3T3-J2 fibroblasts were seeded onto the surface of the polymerized PHH macrogels the next day at a 1:1 ratio with the PHHs (20K cells/well for each cell type in a 24-well plate).

Hepatocyte Functional Assessments

Culture supernatants were assayed for albumin using a sandwich enzyme-linked immunosorbent assay (ELISA; Bethyl Laboratories, Montgomery, TX, USA) with horseradish peroxidase detection and 3,3 ,5,5 - tetramethylbenzidine (TMB; Rockland Immunochemicals, Boyertown, PA, USA) as the substrate[7]. Urea concentration in supernatants was assayed using a colorimetric end point assay utilizing diacetyl monoxime with acid and heat (Stanbio Labs, Boerne, TX, USA)[7]. Absorbance values were quantified on the Synergy H1 multimode plate reader (BioTek, Winooski, VT, USA).

CYP3A4 and CYP2C9 enzyme activities were measured by incubating the cultures with luciferin-IPA or luciferin-H substrates (Promega Life Sciences, Madison, WI, USA) for 3 h, respectively. The metabolite, luciferin, was quantified via luminescence detection on the Synergy H1 multimode plate reader according to the manufacturer's protocols. CYP1A2 and CYP2A6 activities were measured by incubating the cultures with 5 μM 7-ethoxyresorufin or 50 μM coumarin (Sigma-Aldrich) for 3 h, respectively. The metabolites, resorufin and 7-hydroxycoumarin (7-HC), generated from 7-ethoxyresorufin and coumarin, respectively, were quantified via fluorescence

detection (excitation/emission: 550/585 nm for resorufin, and 355/460 nm for 7-HC) on the Synergy H1 multimode plate reader[24].

Gene Expression Analysis

Total cellular RNA was extracted using TRIzol™ (Thermo Fisher Scientific, Waltham, MA, USA), purified using RNeasy mini kit (Qiagen, Germantown, MD, USA), and genomic DNA was digested using Optizyme™ recombinant DNase-I digestion kit (Thermo Fisher) per the manufacturers' instructions. Purified RNA was then reverse transcribed into complementary DNA (cDNA) using the high-capacity cDNA reverse transcription kit (Thermo Fisher) per the manufacturer's instructions on a MasterCycler RealPlex 2 (Eppendorf, Hauppauge, NY, USA). Then 250 ng of cDNA was added to each quantitative polymerase chain reaction (qPCR) along with the TaqMan™ master mix (Thermo Fisher) and predesigned TaqMan human-specific primer/probe sets per the manufacturer's protocols. The primer/probe sets were selected to be human specific without cross-reactivity to mouse DNA and included glyceraldehyde 3-phosphate dehydrogenase (*GAPDH*), CCAAT/enhancer binding protein alpha (*CEBP*a), hepatocyte nuclear factor 4-alpha (*HNF4*a), *albumin*, ornithine transcarbamylase (*OTC*), cytochrome P450 1A2 (*CYP1A2*), *CYP2A6*, *CYP2B6*, *CYP2C8*, *CYP2C9*, *CYP2C19*, *CYP2D6*, *CYP3A4*, multidrug resistance associated protein 2 (*MRP2*), solute carrier organic anion transporter family member 1B1 (*SLCO1B1*), aryl hydrocarbon receptor (*AHR*), constitutive androstane receptor (*CAR*), pregnane X receptor (*PXR*), and retinoid X receptor (*RXR*). TaqMan primer/probe sequences are proprietary to the manufacturer. Hepatic gene expression was normalized to *GAPDH*.

Drug-Mediated CYP Induction and Drug-Induced Hepatotoxicity Studies

Conventional 2D PHH monocultures were allowed 1 day, and PHH/3T3-J2-coated microtissues were allowed 9 days to functionally stabilize, and then both culture models (created from the same PHH lot/donor) were treated with either 6.25 μM rifampin or 3.125 μM omperazole (Sigma-Aldrich) for a total of 4 days with fresh drug added at the 2-day medium exchange. The drug was dissolved in 100% dimethyl sulfoxide (DMSO; Corning Life Sciences). The final DMSO concentration in the culture medium was kept at 0.1% (v/v), and a DMSO-only control culture was used to calculate fold changes due to the drug treatment. After 4 days of drug treatment, CYP3A4 and CYP2C9 activities were measured for rifampin-treated cultures, and CYP1A2 activity was measured for omeprazole-treated cultures as described above.

Additionally, PHH/3T3-J2-coated microtissues were allowed 9 days to functionally stabilize and then treated with either rosiglitazone or troglitazone (Cayman Chemicals, Ann Arbor, MI) at two concentrations for each drug, $30\times$ and $60\times$ C_{max} (C_{max} is the maximum drug concentration measured in human plasma; reported C_{max} for troglitazone and rosiglitazone are 2.82 and 0.373 μg/mL, respectively[25]), for a total of 8 days with fresh drug added to culture medium at the 4-day medium exchange. Previously, 5–9 days of treatment with drugs was found to increase the sensitivity for drug toxicity detection without an increase in the false-positive rate over 1-day drug treatment in 2D PHH/3T3-J2 cocultures[21]. Both drugs were dissolved in 100% DMSO. The final DMSO concentration in the culture medium was kept at 0.1% (v/v) for both drugs, and a DMSO-only control culture was used to calculate fold changes due to the drug treatment. Albumin secretion, as a marker of hepatic dysfunction following drug treatment[21], was measured as described above, while overall viability of the coculture was quantified via the PrestoBlue™ assay (Thermo Fisher) per the manufacturer's instructions. Briefly, PrestoBlue substrate was combined with culture medium at a 1:9 ratio (v/v). The mixture was added to cultures, incubated for 3 h, and the metabolite (resazurin) was quantified via fluorescence detection (excitation/emission: 560/590 nm) on the Synergy H1 multimode plate reader.

Data Analysis

All findings were confirmed in two to three independent experiments (three to four wells per condition and per experiment) from two cryopreserved PHH lots (see section "PHH monocultures" above for deidentified donor information). Data processing was performed using Microsoft Excel, and image analysis was performed using ImageJ[26]. GraphPad Prism (La Jolla, CA, USA) or Mathematica (Wolfram Research, Champaign, IL, USA) was used for displaying results. Mean and standard deviation are displayed for all data sets. Gene expression data in microtissues were calculated as fold changes relative to gene expression data in PHHs immediately following thawing using the C_T method with *GAPDH* as the housekeeping gene. Statistical significance was determined using Student's *t*-test or one-way analysis of variance (ANOVA) followed by a Bonferroni pairwise post hoc test ($p < 0.05$).

RESULTS

Fabrication of PHH Microtissues via Droplet Microfluidics

PHH microtissues were fabricated using droplet microfluidics and seeded into agarose microwells within industry-standard 24-well plates as illustrated in Figure 1a. While a variety of natural ECM materials are compatible with hepatocyte culture[5,13], rat tail collagen I

was selected here for generating microtissues since it is abundantly and cheaply available at high concentrations needed for gelation (>2 mg/ml) and has been utilized extensively for both short-term and long-term PHH culture and PHH/NPC cocultures[5,7]. However, to prevent the aggregation of microtissues before polymerization, microtissues were collected at 37°C directly from the autoclaved microfluidic device (Fig. 1b) to ensure immediate polymerization using a bead bath (Fig. 1c and d). This provided a simple method of polymerizing the microtissues off-chip as opposed to using complicated on-chip heating. The microtissues were collected into an autoclaved 2-ml collection tube, which was directly connected to the microfluidic device with outlet tubing to prevent possible contamination, creating a closed environment between the syringes, microfluidic device, and collection tubes (Fig. 1d). The oil was drained from the collection tube using a syringe, and microtissues were resuspended in culture medium. Finally, to prevent their aggregation during culture, microtissues were placed into agarose microwells cast within each well of a multiwell plate. Agarose was chosen over PDMS or PEG since it is cheaply available, does not typically interact with compounds of diameters <60 nm[27,28], and does not bind to proteins or cells.

Since PHH functions are known to be dependent on homotypic interactions and resulting tight junction formation in 2D cultures[7], here PHHs were mixed with the collagen I at different densities (1.25e6, 2.5e6, 3.75e6, and 5e6 cells/ml) prior to introduction into the droplet microfluidic device. Highly reproducible microtissues were produced with an average diameter of 267.4 μm (standard deviation of 32.7 μm, $n = 375$ microtissues) while containing ~17 and ~34 encapsulated PHHs per microtissue for 1.25e6 (Fig. 2a) and 2.5e6 (Fig. 2b) PHHs/ml densities, respectively. In contrast, microtissues created using the densities of 3.75e6 or 5e6 PHHs/ml produced several larger microtissues that were not the desired diameter and did not fit into the agarose microwells; furthermore, such high cell densities also caused some instability in the oil emulsion, producing a "webbing" of collagen with
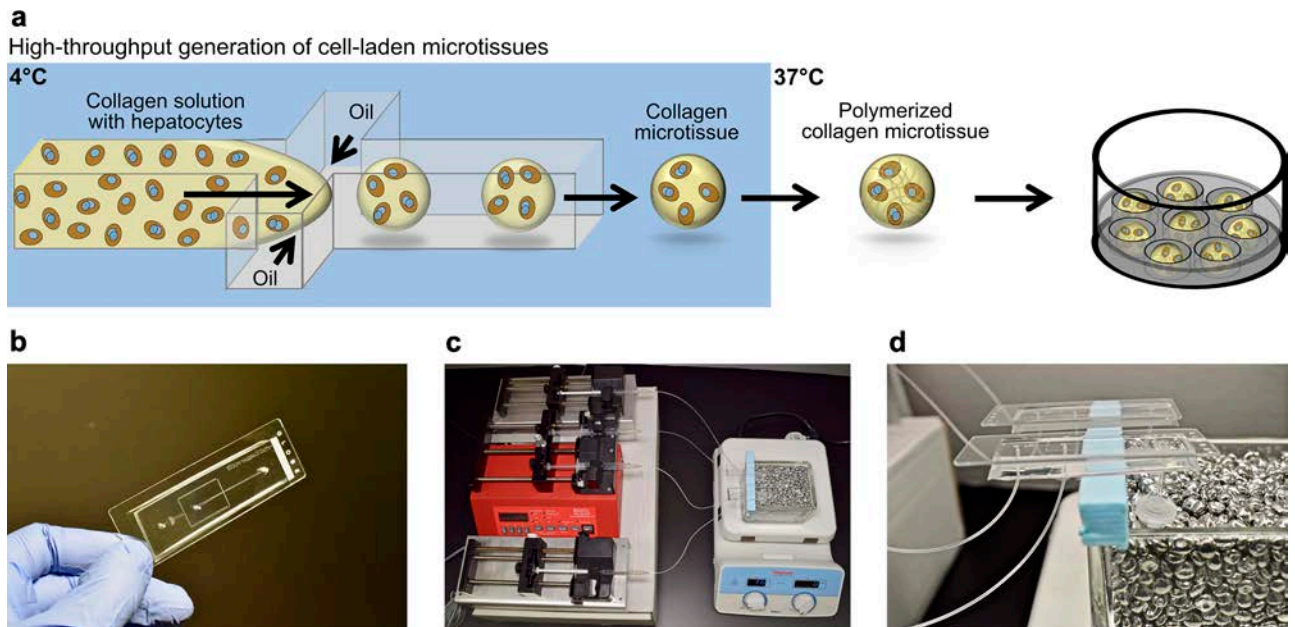
Figure 1. Fabrication of primary human hepatocyte (PHH) microtissues via droplet microfluidics. (a) Hepatocytes are suspended in pH-neutralized collagen solution and then perfused through a droplet generating microfluidic device (see Materials and Methods for details about device dimensions). Oil is perfused at a rate ~4 times faster than the aqueous phase to produce microtissues. Microtissues are formed using the microfluidic device at 4°C and collected at 37°C to promote the rapid polymerization of the collagen droplets and encapsulation of the cells within the droplets. Oil is removed and polymerized microtissues are resuspended in culture medium and subsequently seeded into agarose (2% w/v) microwells cast within multiwell plates. The hepatocytes can be cocultured with nonparenchymal cell (NPC) types by either coencapsulating both cell types within the microtissue or by seeding/coating the NPCs onto the surface of the polymerized collagen-based hepatic microtissues. (b) Polydimethylsiloxane (PDMS)-based microfluidic devices consisting of a single emulsion droplet generator with 300-μm straight channel and 150-μm nozzle used to fabricate microtissues. (c) Microtissue fabrication setup to create microtissues. Two parallel microfluidic devices with syringes containing either oil or collagen + cells are shown; however, additional devices can be run simultaneously to increase fabrication throughput. (d) Microfluidic devices with collection tubes. The microtissues are collected into a 2-ml collection tube connected to the microfluidic device with a short outlet tubing. The collection tube is kept at 37°C in a heated bead bath to ensure immediate polymerization of the microtissues as they are dispensed into the tube.
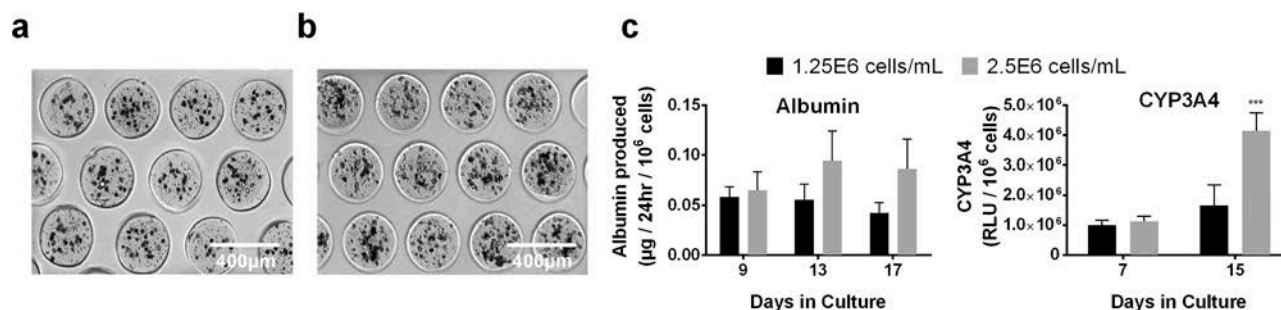
Figure 2. Effects of PHH homotypic interactions within microtissues on liver functions. Collagen-based microtissues containing increasing densities of PHHs in a pH-neutralized collagen (1.25e6 and 2.5e6 cells/ml) solution were fabricated using the droplet microfluidic device shown in Figure 1. Representative phase-contrast images of PHH microtissues with a density of (a) 1.25e6 cells/ml and (b) 2.5e6 cells/ml placed within agarose microwells cast within 24-well plates. Both 1.25e6 and 2.5e6 cells/ml densities produced reproducible microtissues with high yields that fit within the 300 μm × 300 μm agarose microwells. (c) Albumin production and CYP3A4 enzyme activity for PHH microtissues fabricated using a cell density of 1.25e6 and 2.5e6 cells/ml. Microtissues with 3.75e6 and 5e6 cells/ml densities were also fabricated, but these densities did not produce homogenously sized microtissues (not shown). Statistical significance is displayed relative to 1.25e6 cells/ml at the same time point. ***p 0.001.

entrapped PHHs (data not shown). At a functional level, the microtissues created using 2.5e6 PHHs/ml secreted albumin and displayed CYP3A4 activity at ~2- and 2.5-fold higher rates (normalized to cell number), respectively, than microtissues created using 1.25e6 PHHs/ml after 2 weeks (Fig. 2c), thereby showing the positive effects of increased homotypic interactions on hepatic functional output. Thus, the 2.5e6 PHHs/ml density was selected for all subsequent studies with microtissues.

Comparison of PHH Microtissues With Conventional Self-Assembled Spheroids and Macrogels

Microtissues at 2.5e6 PHHs/ml were created as described above (Fig. 3a). Self-assembled spheroids of consistent sizes were created by seeding PHHs directly into the agarose microwells; 200K cells/well (24-well plates) produced tight spheroids with an average diameter of 207.9 μm (standard deviation of 21.3 μm, $n = 375$ microtissues) (Fig. 3b). Lastly, collagen was dispensed directly into multiwell plates to create macrogels with 20K cells/well, a number of cells that is consistent with that present in the microtissues created at 2.5e6 PHHs/ml (Fig. 3c); the collagen hydrogel containing PHHs stably adhered to the plastic plates.

PHHs in microtissues secreted albumin at ~2-fold higher rates than spheroids even with 10-fold fewer cells/volume ratio than the spheroids; similarly, PHHs in microtissues secreted albumin at 4.2- and 30-fold higher rates than macrogels after 13 and 21 days in culture, respectively (Fig. 3d). Comparably, CYP450 (3A4, 2A6, 2C9, and 1A2) enzyme activities were higher in microtissues than both the spheroids and macrogels. For CYP3A4, microtissues outperformed spheroids by 6.1- and 3.4-fold after 13 and 21 days, respectively; similarly, microtissues outperformed macrogels by 2.7- and 4.8-fold at the

same time points above (Fig. 3e). For CYP2A6, microtissues outperformed spheroids by 6.9- and 2.6-fold after 13 and 21 days, respectively; similarly, microtissues outperformed macrogels by 1.4-fold after 21 days (Fig. 3f). For CYP2C9, microtissues outperformed spheroids by 2.6- and 1.5-fold after 13 and 21 days, respectively; macrogels, on the other hand, had undetectable levels of CYP2C9 activity (Fig. 3g). Finally, for CYP1A2, microtissues outperformed spheroids by 1.2- and 6-fold after 13 and 21 days, respectively; macrogels, on the other hand, had undetectable levels of CYP1A2 activity (Fig. 3h).

Overall, PHH-only spheroids functionally outperformed PHH-only macrogels for CYP1A2/CYP2C9 activities and albumin secretion, while macrogels outperformed spheroids for CYP3A4/CYP2A6 activities. On the other hand, microtissues outperformed both spheroids and macrogels across all measured functions as discussed above.

Effects of 3T3-J2 Murine Embryonic Fibroblasts and Primary Human HSCs on PHH Microtissues

3T3-J2 fibroblasts are known to enhance PHH functions in both 2D cocultures[7] and 3D self-assembled spheroids[20]. Therefore, here PHHs and growth-arrested 3T3-J2 fibroblasts (1:1) were either coencapsulated within the microtissue or fibroblasts were "coated" onto the surface of the collagen-based PHH microtissues and compared to PHH-only microtissues (Fig. 4a–c). In contrast to PHH-only microtissues, 3T3-J2-coencapsulated microtissues and 3T3-J2-coated microtissues were compacted by ~50% due to the fibroblasts. Specifically, 3T3-J2-coencapsulated microtissues and 3T3-J2-coated microtissues were compacted to an average diameter of 149.2 μm (standard deviation of 22.6 μm, $n = 375$ microtissues) and 140.4 μm (standard deviation of 13.4 μm, $n = 375$ microtissues), respectively (Fig. 7).
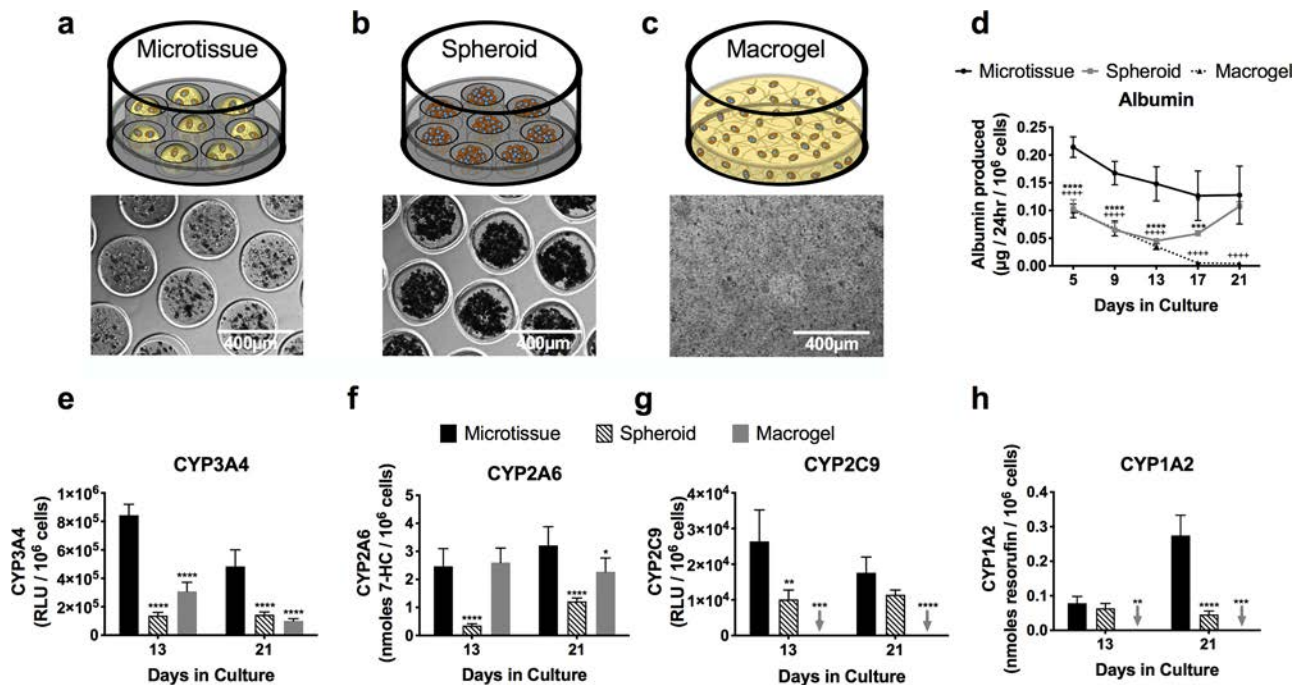
Figure 3. Comparison of PHH microtissues with conventional self-assembled spheroids and macrogels. Schematics and phase-contrast images for the tested culture models: (a) microtissue containing collagen and PHHs formed using the droplet microfluidic device of Fig. 1; (b) self-assembled PHH spheroids without any collagen scaffolding; (c) macrogels in which the PHH + collagen mixture is dispensed directly into multiwell plates without being subjected to a droplet microfluidic device. (d) Albumin production from PHH-only microtissues, spheroids, and macrogels. Statistical significance is displayed for microtissues relative to spheroids (***p 0.001, and ****p 0.0001) and for microtissues relative to macrogels (++++p 0.0001). Activities of different CYP450 isoenzymes (e) CYP3A4, (f) CYP2A6, (g) CYP2C9, and (h) CYP1A2 in PHH-only microtissues, spheroids, and macrogels. Statistical significance is displayed relative to microtissues at the same time point. *p 0.05, **p 0.01, ***p 0.001, and ****p 0.0001. Arrows indicate undetectable levels for the indicated function and indicated culture model.

At a functional level, albumin secretion rates were ~5-fold higher in the 3T3-J2-coencapsulated microtissues than PHH-only microtissues after 20 days in culture (Fig. 4e). For CYP3A4, 3T3-J2-coencapsulated microtissues outperformed PHH-only microtissues by threefold after 12 and 20 days (Fig. 4f). For CYP2A6, 3T3-J2-coencapsulated microtissues outperformed PHH-only microtissues by 2.8- and 4.4-fold after 12 and 20 days, respectively (Fig. 4g). For CYP2C9, 3T3-J2-coencapsulated microtissues outperformed PHH-only microtissues by 2.7- and 4-fold after 12 and 20 days, respectively (Fig. 4h). However, for CYP1A2, PHH-only microtissues outperformed 3T3-J2-coencapsulated microtissues by 1.6-fold after 20 days (Fig. 4i). Fibroblasts were found to be devoid of any of the measured liver functions, including albumin secretion, urea synthesis, and CYP450 activities (data not shown).

3T3-J2-coated microtissues functionally outperformed both 3T3-J2-coencapsulated and PHH-only microtissues. For albumin, 3T3-J2-coated microtissues outperformed coencapsulated ones by 5- and 4.2-fold after 8 and 24 days, respectively; similarly, 3T3-J2-coated microtissues outperformed PHH-only microtissues by 4.2- and 20.6-fold at the same time points above (Fig. 4e). For CYP3A4, 3T3-J2-coated microtissues outperformed coencapsulated ones by 1.3- and 2.7-fold after 12 and 20 days, respectively; similarly, 3T3-J2-coated microtissues outperformed PHH-only microtissues by 3.8- and 8-fold at the same time points above (Fig. 4f). For CYP2A6, 3T3-J2-coated microtissues outperformed coencapsulated ones by 4.5-fold after 20 days; similarly, 3T3-J2-coated microtissues outperformed PHH-only microtissues by 2.4- and 19.5-fold after 12 and 20 days, respectively (Fig. 4g). For CYP2C9, 3T3-J2-coated microtissues outperformed coencapsulated ones by 2- and 3.7-fold after 12 and 20 days, respectively; similarly, 3T3-J2-coated microtissues outperformed PHH-only microtissues by 6- and 7.6-fold at the same time points above (Fig. 4h). Lastly, for CYP1A2, 3T3-J2-coated microtissues outperformed coencapsulated ones by 1.8-fold after 20 days; similarly, 3T3-J2-coated microtissues outperformed PHH-only microtissues by 3.4-fold after 12 days, although functions across the two models were similar after 20 days (Fig. 4i).
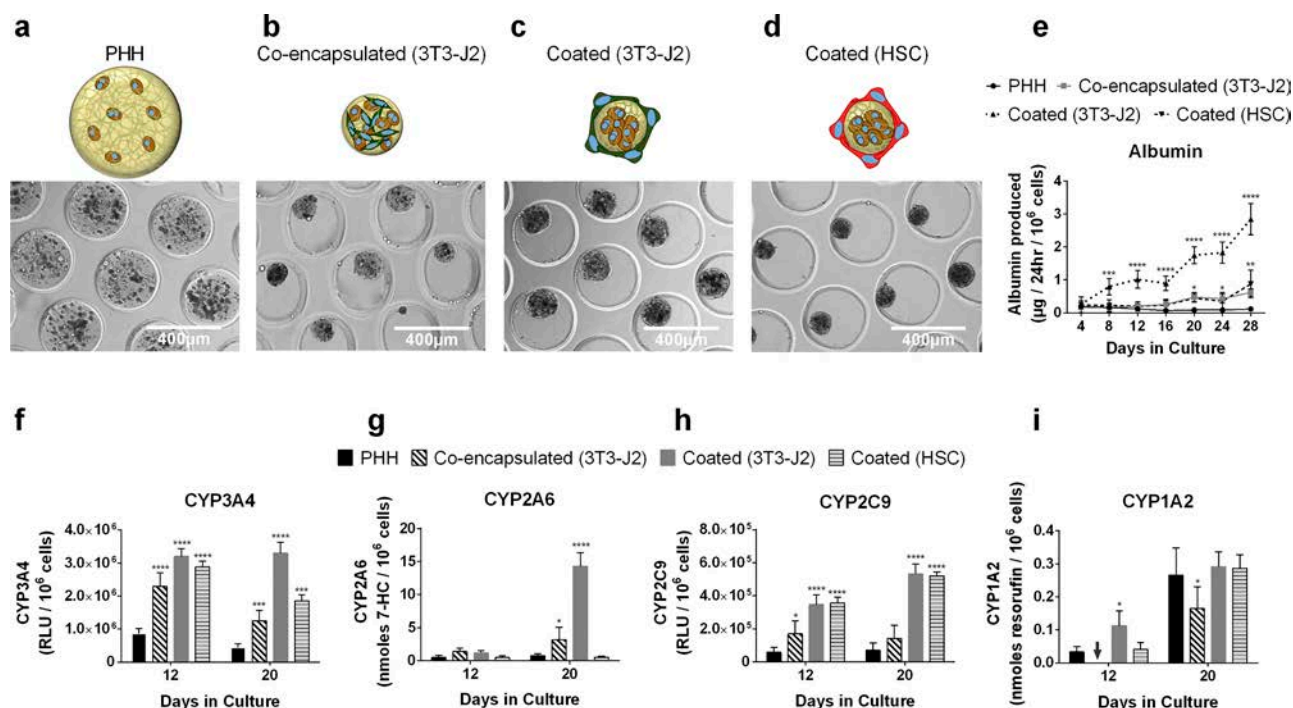
Figure 4. Effects of 3T3-J2 fibroblasts and primary human hepatic stellate cells (HSCs) on PHH microtissues. Phase-contrast images for tested culture models: (a) Only PHHs encapsulated within collagen microtissues; (b) PHHs and 3T3-J2 fibroblasts encapsulated together within the collagen microtissue [coencapsulated (3T3-J2)]; (c) 3T3-J2 fibroblasts seeded/coated onto the surface of the polymerized collagen-based PHH microtissues [coated (3T3-J2)]; (d) primary HSCs seeded/coated onto the surface of the polymerized collagen-based microtissues [coated (HSC)]. The smaller size of the microtissues with coculture indicate compaction of the microtissues by the fibroblasts. (e) Albumin secretions from PHH-only, PHH/3T3-J2-coencapsulated, PHH/3T3-J2-coated, and PHH/HSC-coated microtissues. Activities of different CYP450 isoenzymes, (f) CYP3A4, (g) CYP2A6, (h) CYP2C9, (i) CYP1A2 in PHH-only, PHH/3T3-J2-coencapsulated, PHH/3T3-J2-coated, and PHH/HSC-coated microtissues. Statistical significance is displayed relative to PHH-only microtissues (*p 0.05, **p 0.01, ***p 0.001, ****p 0.0001). Arrow indicates undetectable level for the indicated function and indicated culture model.

Primary HSCs differentiated into myofibroblasts via passaging onto tissue culture plastic have been shown to promote PHH function in 2D culture, albeit at lower levels than 3T3-J2 fibroblasts[23], although effects in 3D remain undetermined. Therefore, here HSCs were coated onto PHH microtissues to determine functional effects in 3D (Fig. 4d). HSC-coated microtissues had 5- and 7.4-fold higher albumin secretion rates than PHH-only microtissues after 20 and 28 days in culture, respectively; however, 3T3-J2-coated microtissues had 3.9- and 3.3-fold higher albumin secretion rates than HSC-coated microtissues at the same time points above (Fig. 4e). For CYP3A4, HSC-coated microtissues outperformed PHH-only microtissues by 3.3- and 4.2-fold after 12 and 20 days, respectively; however, 3T3-J2-coated microtissues outperformed HSC-coated microtissues by 1.8-fold after 20 days (Fig. 4f). For CYP2A6, unlike 3T3-J2-coated microtissues that upregulated enzymatic activity relative to PHH-only microtissues by up to 19.5-fold on day 20, HSC-coated microtissues did not display enhanced CYP2A6 activity relative to PHH-only microtissues (Fig.

4g). For CYP2C9, similar to 3T3-J2-coated microtissues, HSC-coated microtissues outperformed PHH-only microtissues by 6.2- and 7.5-fold after 12 and 20 days, respectively (Fig. 4h). Lastly, for CYP1A2, HSC-coated microtissues had similar enzymatic activity as compared to PHH-only microtissues, whereas the 3T3-J2-coated microtissues showed a transient upregulation after 12 days in culture relative to HSC-coated microtissues (Fig. 4i).

Overall, 3T3-J2-coated microtissues functionally outperformed HSC-coated microtissues in albumin secretion and three out of the four CYP enzyme activities measured (CYP3A4, CYP2A6, and CYP1A2). Therefore, 3T3-J2-coated microtissues were utilized for subsequent studies.
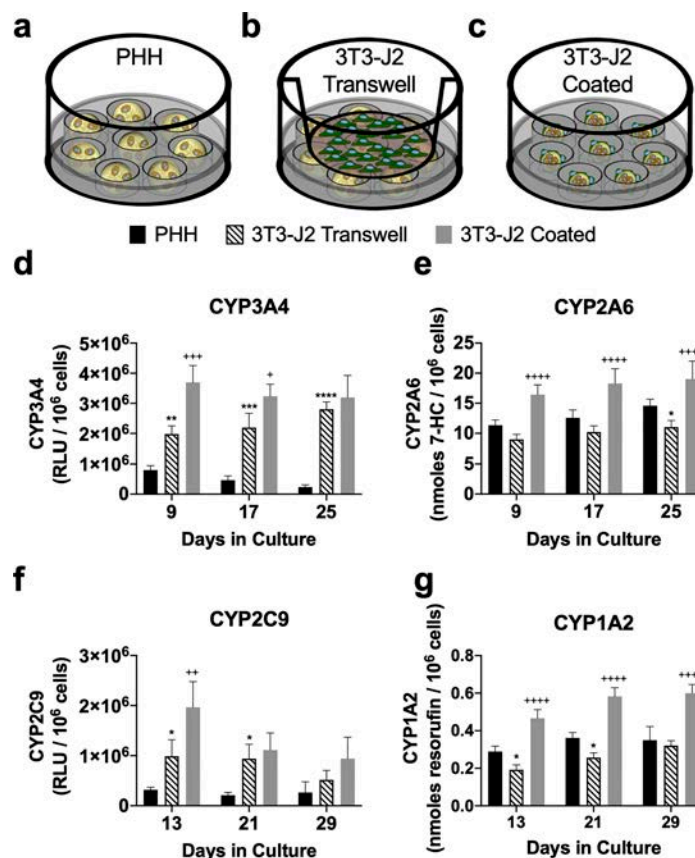
Effects of Paracrine-Only Interactions Between 3T3-J2 Fibroblasts and PHH Microtissues

As discussed above, 3T3-J2 fibroblasts were shown to enhance PHH functions to the highest degree when the fibroblasts were coated onto the surface of the microtissues as compared to when both cell types were coencapsulated into the collagen gels; however, it is unclear if

paracrine secretions from the fibroblasts alone are sufficient to induce maximal functions in the microtissues containing PHHs. Therefore, PHH-only microtissues were placed into agarose microwells within a 24-well plate, and then 3T3-J2 fibroblasts were seeded into a Transwell insert placed within the well (3T3-J2 Transwell) (Fig. 5b). Hepatic functions in 3T3-J2 Transwell microtissues were compared against PHH-only (Fig. 5a) microtissues without any fibroblast influence and 3T3-J2-coated microtissues containing PHHs (Fig. 5c). For CYP3A4, 3T3-J2 Transwell microtissues outperformed PHH-only microtissues by 2.5-, 4.7-, and 11.8-fold after 9, 17, and 25 days, respectively (Fig. 5d). For CYP2A6, 3T3-J2 Transwell microtissues did not display enhanced CYP2A6 activity relative to PHH-only microtissues (Fig. 5e). For CYP2C9, 3T3-J2 Transwell microtissues outperformed PHH-only microtissues by 3.1-, 4.4-, and 1.95-fold after 13, 21, and 29 days, respectively (Fig. 5f). For

CYP1A2, 3T3-J2 Transwell microtissues did not display enhanced CYP1A2 activity relative to PHH-only microtissues (Fig. 5g).

In contrast, 3T3-J2-coated microtissues functionally outperformed both 3T3-J2 Transwell and PHH-only microtissues. For CYP3A4, 3T3-J2-coated microtissues outperformed Transwell ones by 1.9- and 1.5-fold after 9 and 17 days, respectively; however, similar activity was observed on day 25 (Fig. 5d). Similarly, for CYP3A4, 3T3-J2-coated microtissues outperformed PHH-only microtissues by 4.6-, 7-, and 13.5-fold after 9, 17, and 25 days, respectively. For CYP2A6, 3T3-J2-coated microtissues outperformed Transwell ones by 1.8-, 1.8-, and 1.7-fold after 9, 17, and 25 days, respectively; similarly, 3T3-J2-coated microtissues outperformed PHH-only microtissues by 1.4-, 1.5-, and 1.3-fold at the same time points above (Fig. 5e). For CYP2C9, 3T3-J2-coated microtissues outperformed Transwell ones by 2- and 1.8-fold after 13

Figure 5. Effects of paracrine-only interactions between 3T3-J2 fibroblasts and PHH microtissues. Schematics for tested culture models: (a) Only PHHs encapsulated within collagen microtissues (control model); (b) PHH microtissues with 3T3-J2 fibroblasts seeded into a Transwell insert (3T3-J2 Transwell); (c) 3T3-J2 fibroblasts coated onto the surface of the polymerized collagen-based PHH microtissues (3T3-J2 coated, control model). Activities of different CYP450 isoenzymes, (d) CYP3A4, (e) CYP2A6, (f) CYP2C9, (g) CYP1A2 in PHH-only, 3T3-J2 Transwell, and 3T3-J2-coated microtissues. Statistical significance is displayed for 3T3-J2 Transwell microtissues relative to PHH-only microtissues (*p 0.05, **p 0.01, ***p 0.001, ****p 0.0001). Statistical significance is displayed for 3T3-J2-coated microtissues relative to 3T3-J2 Transwell microtissues (+p 0.05, ++p 0.01, +++p 0.001, ++++p 0.0001).

and 29 days, respectively; however, similar activity was observed on day 21 (Fig. 5f). Similarly, 3T3-J2-coated microtissues outperformed PHH-only microtissues by 6.2-, 5.2-, and 3.5-fold after 13, 21, and 29 days, respectively. For CYP1A2, 3T3-J2-coated microtissues outperformed Transwell ones by 2.4-, 2.3-, and 1.9-fold after 13, 21, and 29 days, respectively; similarly, 3T3-J2-coated microtissues outperformed PHH-only microtissues by 1.6-, 1.6-, and 1.7-fold at the same time points above (Fig. 5g). Finally, 3T3-J2 Transwell microtissues secreted higher levels of albumin than PHH-only microtissues over 6 weeks but still lower (~25%–63%) than those secreted by the 3T3-J2-coated microtissues (data not shown).

Overall, secretions from 3T3-J2 fibroblasts in Transwells were able to induce some hepatic functions (CYP3A4, CYP2C9, and albumin); however, additional CYP enzymes were not improved from paracrine signaling alone. On the other hand, coating 3T3-J2 fibroblasts onto the PHH-containing microtissues was able to induce all the measured functions as compared to PHH-only microtissues.

Comparison of 3T3-J2-Coated Microtissues With Similarly Coated Self-Assembled Spheroids and Coated Macrogels

As with coated microtissues (Fig. 6a), 3T3-J2 fibroblasts were coated onto self-assembled PHH spheroids (1:1 ratio between the two cell types) (Fig. 6b), and such coated spheroids were also compacted by ~35% due to the fibroblasts with an average diameter of 133.7 μm (standard deviation of 21.6 μm, $n = 375$ microtissues); however, coated microtissues had a more consistent size distribution than coated spheroids (Fig. 7). Similarly, 3T3-J2 fibroblasts were coated onto the surface of PHH macrogels at a 1:1 ratio (Fig. 6c).

At a functional level, coated microtissues outperformed both coated spheroids and coated macrogels. For albumin secretion, coated microtissues outperformed coated spheroids by 2-fold and 2.3-fold after 13 and 21 days, respectively; similarly, coated microtissues outperformed coated macrogels by 22.9- and 36.2-fold at the same time points above (Fig. 6d). For CYP3A4, coated microtissues outperformed coated spheroids by 5.6- and 4-fold after 13 and 21 days, respectively; similarly, coated microtissues outperformed coated macrogels by 7.6- and 19.1-fold (Fig. 6e). For CYP2A6, coated microtissues outperformed coated spheroids by 2.5- and 3.7-fold after 13 and 21 days, respectively; similarly, coated microtissues outperformed coated macrogels by 1.3- and 3.7-fold (Fig. 6f). For CYP2C9, coated microtissues outperformed coated spheroids by 3.3- and 3.4-fold after 13 and 21 days, respectively; similarly, coated microtissues
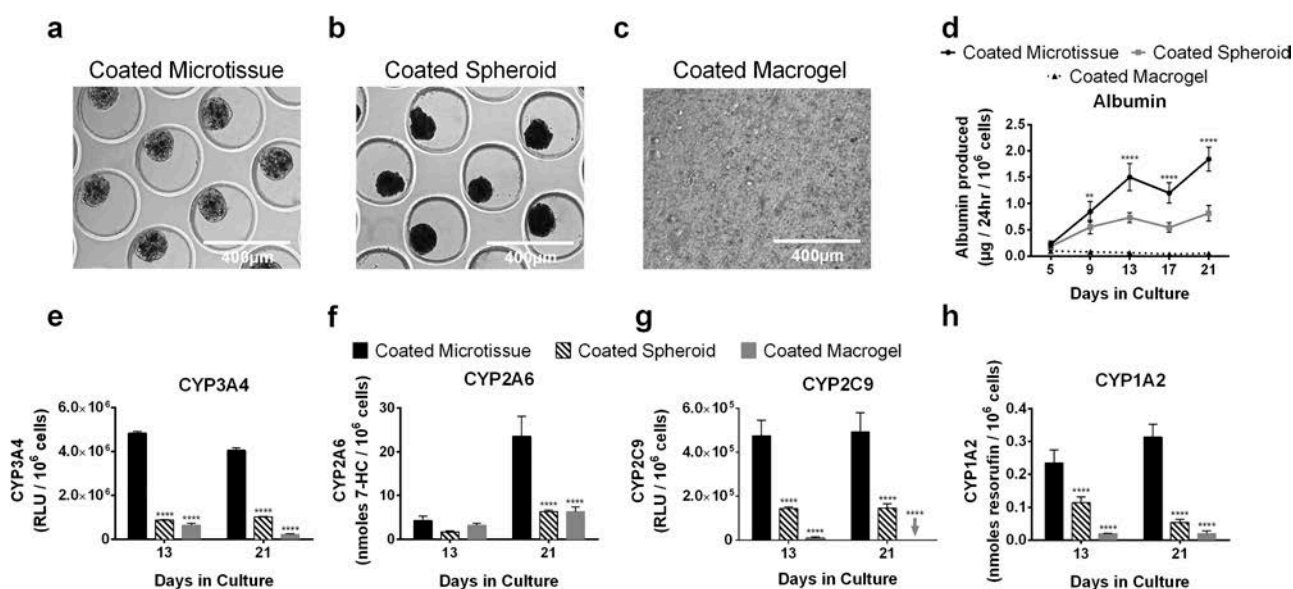
Figure 6. Comparison of 3T3-J2-coated microtissues with similarly coated self-assembled spheroids and coated macrogels. (a) 3T3-J2 fibroblasts were coated onto the surface of the polymerized collagen-based PHH microtissues (coated microtissue). (b) Similarly, self-assembled PHH spheroids were coated with 3T3-J2 fibroblasts (coated spheroids), and (c) macrogels were coated with 3T3-J2 fibroblasts (coated macrogels). (d) Albumin production in the coated microtissues, coated spheroids, and coated macrogels. Statistical significance is displayed for coated microtissues relative to coated spheroids at the same time point (**p 0.01, and ****p 0.0001). Activities of different CYP450 isoenzymes, (e) CYP3A4, (f) CYP2A6, (g) CYP2C9, and (h) CYP1A2 in the coated microtissues, coated spheroids, and coated macrogels. Statistical significance is displayed for coated spheroids and coated macrogels relative to coated microtissues at the same time point (****p 0.0001). Arrow indicates undetectable level for the indicated function and indicated culture model.
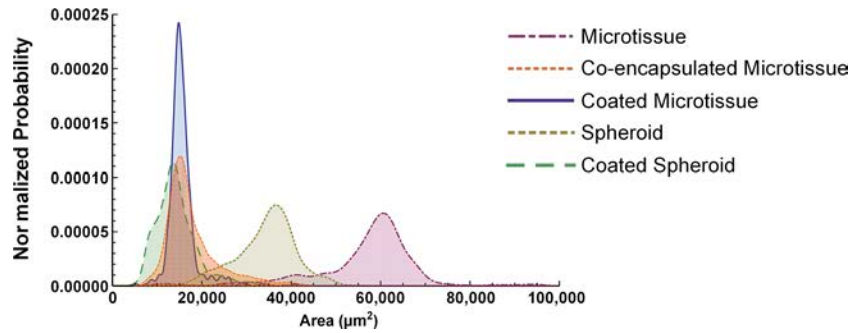
Figure 7. Projected surface area distributions of 3D human liver models. Collagen-based microtissues containing encapsulated PHHs were fabricated using the droplet microfluidic device shown in Figure 1, while self-assembled spheroids were created as shown in Figure 3. Collagen-based microtissues containing encapsulated PHHs and 3T3-J2 fibroblasts were fabricated to create coencapsulated microtissue. 3T3-J2 fibroblasts were coated onto the PHH microtissues or spheroids to create coated microtissue and coated spheroid, respectively. Spheroid and Microtissue indicate models with only PHHs. After 21 days of culture, 375 individual constructs for each model were fixed and analyzed via phase-contrast microscopy for projected surface area determinations. Shown here are the histograms of the projected surface areas for the five culture/coculture models.

outperformed coated macrogels by 54-fold after 13 days, while CYP2C9 activity was undetectable in macrogels after 21 days (Fig. 6g). Finally, for CYP1A2, coated microtissues outperformed coated spheroids by 2- and 5.8-fold after 13 and 21 days, respectively; similarly, coated microtissues outperformed coated macrogels by 12- and 15.7-fold (Fig. 6h).

Overall, coated spheroids functionally outperformed coated macrogels, with CYP2A6 being the sole exception. On the other hand, coated microtissues outperformed both coated spheroids and coated macrogels.

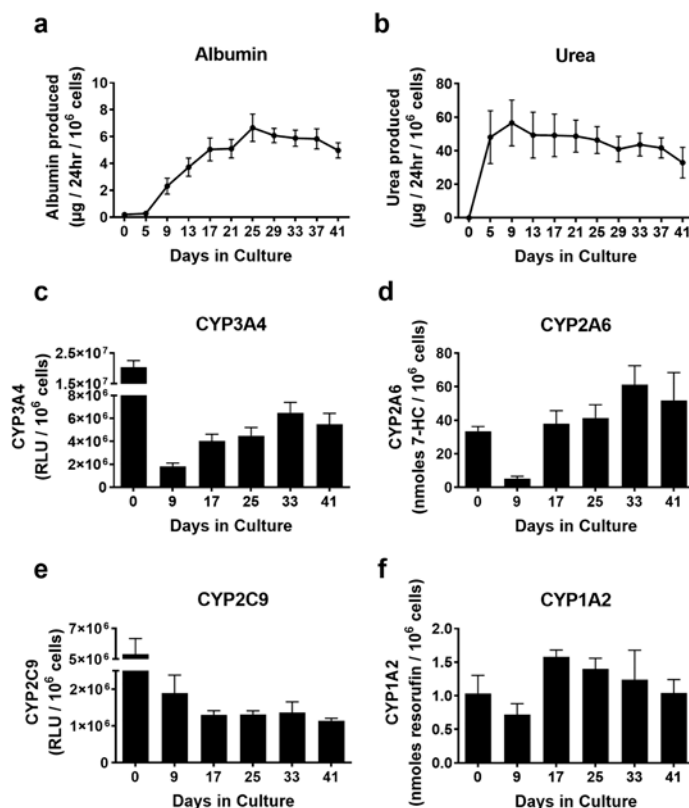*Long-Term Functions in 3T3-J2-Coated Microtissues*

3T3-J2-coated microtissues were assessed for functions over 6 weeks, and these functions were compared to functions in PHHs within 2–4 h of thawing (day 0) as the routinely used culture model for short-term (acute) assays before PHHs severely decline in functions in conventional 2D monoculture formats[5,13]. Albumin secretion was minimal in PHHs on day 0 but ramped up over the first 3 weeks in coated microtissues to ~6 μg/day/million PHHs and remained relatively stable until day 41 when the cultures were sacrificed (Fig. 8a). Urea secretion was undetectable in PHHs on day 0 but increased in coated microtissues over the first 9 days to ~57 μg/day/million PHHs and remained statistically stable for 41 days (Fig. 8b). CYP3A4 activity in the coated microtissues was ~9% of day 0 activity after 9 days and increased to ~20% to 32% for the remaining culture duration (Fig. 8c). CYP2A6 activity in the coated microtissues was ~15% of day 0 activity after 9 days and increased to ~113% to 183% for the remaining duration (Fig. 8d). CYP2C9 activity in the coated microtissues was ~36% of day 0 activity after 9 days and decreased to ~21% to 26% for the remaining culture duration (Fig. 8e). Lastly, CYP1A2

activity in the coated microtissues was ~70% of day 0 activity after 9 days and increased to ~100% to 153% for the remaining duration (Fig. 8f).

Long-Term Gene Expression in 3T3-J2-Coated and HSC-Coated Microtissues

Expression levels of major liver-specific genes, including *albumin*, *OTC*, master transcription factors (*CEBP*a and *HNF4*a), CYP450 enzymes (*CYP1A2, CYP2A6, CYP2B6, CYP2C8, CYP2C9, CYP2C19, CYP2D6,* and *CYP3A4*), drug transporters (*MRP2* and *SLCO1B1*), and nuclear receptors (*AHR, CAR, PXR,* and *RXR*) were characterized in the 3T3-J2-coated microtissues after 2, 4, and 6 weeks following culture initiation (Fig. 9a). Gene expression in the 3T3-J2-coated microtissues was normalized to human *GAPDH* and further normalized to gene expression data in PHHs immediately following thawing (day 0). The expression levels of 13 of the 18 genes were higher in the 3T3-J2-coated microtissues over 6 weeks than the levels in freshly thawed PHHs (e.g., after 6 weeks, 5.8-, 2.6-, 2.9-, 2.1-, 22-, 6-, 1.6-, 1.5-, 2.4-, 73-, 11.4-, 9.3-, and 10.3-fold higher levels in 3T3-J2-coated microtissues than freshly thawed PHHs for *OTC*, *CEBP*a, *HNF4*a, *CYP1A2, CYP2A6, CYP2B6, CYP2C19, CYP2D6, CYP3A4, MRP2, PXR*, and *RXR*, respectively). In contrast, *albumin, CYP2C9, SLCO1B1, AHR,* and *CAR* levels were downregulated in the 3T3-J2-coated microtissues in comparison to freshly thawed PHHs (e.g., after 6 weeks, 55%, 58%, 77%, 63%, and 85% retention in 3T3-J2-coated microtissues of freshly thawed PHH levels, respectively).

Similarly, expression levels of the same liver-specific genes analyzed above were characterized in HSC-coated microtissues containing PHHs (which also upregulated functions compared to PHH-only microtissues, albeit to a

Figure 8. Long-term functions in 3T3-J2-coated microtissues. 3T3-J2 fibroblasts were coated onto the surface of the polymerized collagen-based PHH microtissues ("coated microtissue") and cultured for ~6 weeks. (a) Albumin production, (b) urea production, and the activities of different CYP450 isoenzymes, (c) CYP3A4 activity, (d) CYP2A6, (e) CYP2C9, and (f) CYP1A2 in coated microtissues over time.

less extent than 3T3-J2-coated microtissues, as discussed above). The expression levels of 10 of the 18 genes were generally higher in the HSC-coated microtissues over 6 weeks than the levels in freshly thawed PHHs (Fig. 9b) (e.g., after 6 weeks, 5.1-, 1.2-, 7.5-, 3.9-, 2.2-, 1.6-, 1.1-, 2.7-, 8.8-, and 442.6-fold higher levels in HSC-coated microtissues than freshly thawed PHHs for *OTC*, *CEBP*a, *CYP1A2*, *CYP2A6*, *CYP2B6*, *CYP2C9*, *CYP3A4*, *AHR*, *CAR*, *and RXR*, respectively). In contrast, *albumin*, *CYP2C8*, *CYP2C19*, *CYP2D6*, *MRP2*, *SLCO1B1*, *and PXR,* were downregulated or entirely undetectable in the HSC-coated microtissues after 6 weeks of culture in comparison to freshly thawed PHHs (e.g., after 6 weeks, *albumin* at 0.2%, *CYP2D6* at 22%, and rest of the genes—*CYP2C8, CYP2C19, MRP2, SLCO1B1, PXR*—were undetectable).

Overall, the expression levels for 13 of the 18 genes were higher after 6 weeks in 3T3-J2-coated microtissues as compared to HSC-coated microtissues (i.e., *albumin*, *OTC*, *CEBP*a, *HNF4*a, *CYP2A6*, *CYP2B6*, *CYP2C8*, *CYP2C19*, *CYP2D6*, *CYP3A4*, *MRP2*, *SLCO1B1*, and *PXR*). In comparison, the expression levels of 5 of the

18 genes were higher in HSC-coated microtissues than 3T3-J2-coated microtissues after 6 weeks (i.e., *CYP1A2*, *CYP2C9*, *AHR*, *CAR*, and *RXR*). Importantly, the expression of several critical liver genes (*CYP2C8*, *CYP2C19*, *MRP2*, *SLCO1B1*, and *PXR*) was undetectable after 6 weeks in HSC-coated microtissues but still detectable in the 3T3-J2-coated microtissues.

Drug-Mediated CYP Induction in 2D PHH Monocultures and 3T3-J2-Coated Microtissues

2D PHH monocultures were allowed 1 day and 3T3-J2-coated microtissues containing PHHs were allowed 9 days to functionally stabilize, and then both culture models were treated with rifampin or omeprazole for a total of 4 days with fresh drug added at the 2-day medium exchange. CYP3A4 and CYP2C9 activities were assessed in the rifampin-treated cultures, whereas CYP1A2 activity was assessed in the omeprazole-treated cultures; DMSO-treated control cultures were used to calculate fold changes in induction of CYP activities due to drug treatment. In 2D monocultures, rifampin caused ~5.5-fold induction in CYP3A4 activity and ~1.4-fold induction in CYP2C9
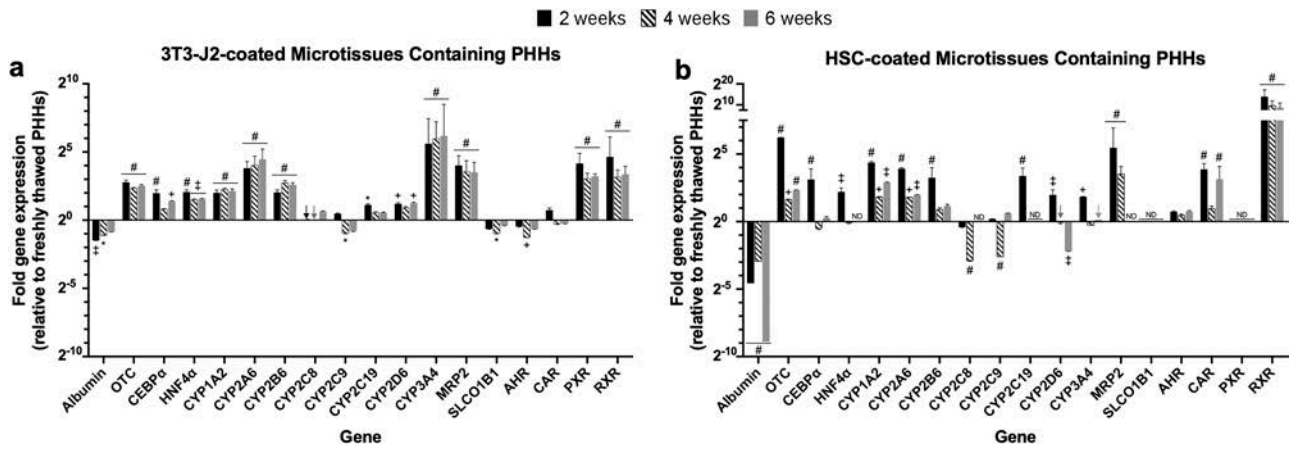
Figure 9. Long-term gene expression in 3T3-J2-coated and HSC-coated microtissues. 3T3-J2 fibroblasts or primary human HSCs were coated onto the surface of the polymerized collagen-based PHH microtissues and cultured for ~6 weeks. Quantitative gene expression of *albumin,* ornithine transcarbamylase (*OTC*), hepatic transcription factors (*CEBPα* and *HNF4α*), CYP enzymes (*CYP1A2, CYP2A6, CYP2B6, CYP2C8, CYP2C9, CYP2C19, CYP2D6,* and *CYP3A4*), canalicular transporter (*MRP2*), basolateral transporter (*SLCO1B1*), and nuclear receptors (*AHR, CAR, PXR,* and *RXR*) in 3T3-J2-coated microtissues (a) and HSC-coated microtissues (b) at 2, 4, and 6 weeks as compared to freshly thawed PHHs (line 2^0) that were immediately lysed in suspension for RNA (i.e., expression levels in the coated microtissues at the 2^0 line are near identical to the levels in freshly thawed PHHs). Arrows indicate detectable levels at the 2^0 line. For expression levels denoted ND (not detectable), amplification was not observed for the given gene within 40 cycles of quantitative polymerase chain reaction (qPCR). Statistical significance for gene expression levels is displayed for 3T3-J2 coated and HSC coated at 2, 4, and 6 weeks relative to freshly thawed PHHs (*p 0.05, +p 0.01, ‡p 0.001, #p 0.0001).

activity relative to the DMSO control, while omeprazole caused ~4-fold induction in CYP1A2 activity (Fig. 10a). In 3T3-J2-coated microtissues, rifampin caused ~7-fold induction in CYP3A4 activity and ~5-fold induction in CYP2C9 activity relative to the DMSO control, while omeprazole caused ~2-fold induction in CYP1A2 activity (Fig. 10a).
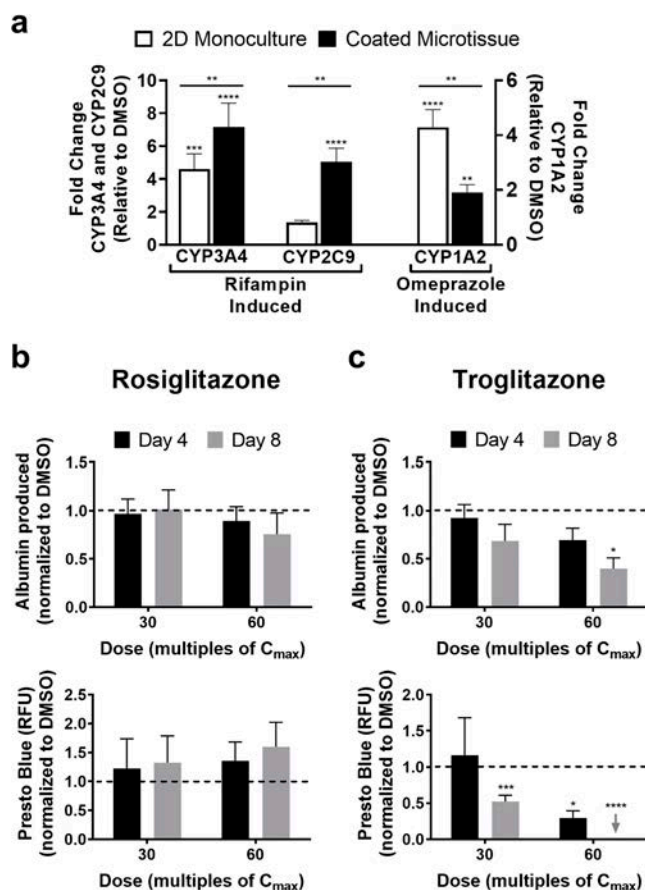
Drug-Induced Hepatotoxicity in 3T3-J2-Coated Microtissues

3T3-J2-coated microtissues stabilized over 9 days were treated with two drugs for type 2 diabetes mellitus, rosiglitazone or troglitazone, at two concentrations for each drug, 30× and 60× C_{max} (C_{max}: maximum drug concentration measured in human plasma), for a total of 8 days with fresh drug added at the 4-day medium exchange. Rosiglitazone is a nonhepatotoxin, while troglitazone was withdrawn from the market due to severe hepatotoxicity[29]. Albumin secretion (hepatocyte marker) and overall coculture viability (metabolism of PrestoBlue™) were assessed after 4 and 8 days of drug treatment, and the data were normalized to the data in DMSO-only treated cultures. No statistically significant downregulation of either albumin or viability was observed in coated microtissues treated with rosiglitazone (Fig. 10b). In contrast, coated microtissues treated with troglitazone displayed time- and concentration-dependent decreases in albumin and viability (Fig. 10c). Albumin secretion declined to 92% and 69% of DMSO-only controls after treatment of

coated microtissues with 30× C_{max} of troglitazone for 4 and 8 days, respectively, whereas it declined to 69% and 40% after treatment with 60× C_{max} at the same time points above. Similarly, viability declined to 29% of DMSO controls after treatment of coated microtissues with 30× C_{max} of troglitazone for 8 days, whereas it declined to 52% after treatment with 60× C_{max} for 4 days and was undetectable following treatment with this concentration for 8 days.

DISCUSSION

In contrast to a limited application scope of 2D models, human liver models that are 3D in architecture have utility not only for preclinical drug development but also for elucidating the reorganization of cell–cell and cell–ECM interactions in liver disease and as building blocks for cell-based therapies in the clinic. In the absence of a functional vasculature, it is important to restrict the size of the 3D human liver models to ~300 μm in diameter to allow for adequate oxygen and nutrient transfer. While such miniaturized models can be created using specialized plates that allow spheroid generation, typically the throughput of such approaches is limited. In contrast, droplet microfluidics provides the ability to rapidly create highly reproducible microtissues containing one or more cell types; however, the use of this technology has been restricted to PHH models containing alginate or PEG that are short-lived (~1 week). Thus, here we utilized droplet microfluidics to create 3D human liver microtissues within a natural collagen-based hydrogel

Figure 10. Drug-mediated CYP induction and drug-induced hepatotoxicity in 3T3-J2-coated microtissues. Coated microtissues were allowed 9 days while 2D PHH monocultures were allowed 1 day to functionally stabilize, and then both culture models (same PHH donor/lot) were treated with rifampin or omeprazole for 4 days with fresh drug added to the culture medium at the 2-day medium exchange. CYP activities were assessed at the end of the 4-day incubation period. (a) CYP3A4 and CYP2C9 activities in 2D monocultures and coated microtissues treated with rifampin, and CYP1A2 activity in 2D monocultures and coated microtissues treated with omeprazole. Enzyme activities in the drug-treated cultures were normalized to enzyme activity in cultures treated with DMSO alone. Statistical significance directly above each bar is displayed relative to DMSO-treated controls (**p 0.01, ***p 0.001, and ****p 0.0001). Statistical significance above each line is displayed for coated microtissue induction relative to 2D monoculture induction (**p 0.01). Additionally, coated microtissues were allowed ~9 days to functionally stabilize and then treated with rosiglitazone or troglitazone at two concentrations for each drug, 30× and 60× C_{max} (C_{max} = maximum drug concentration measured in human plasma; C_{max} for troglitazone = 2.82 μg/ml and C_{max} for rosiglitazone = 0.373 μg/ml), for a total of 8 days with fresh drug added to culture medium at the 4-day medium exchange. (b) Albumin secretion, specific to PHHs (top graph), and overall coculture viability (bottom graph, PrestoBlue™ conversion to the metabolite, resazurin) in coated microtissues treated with rosiglitazone. Data in drug-treated coated microtissues were normalized to the corresponding data in DMSO-only treated cultures. (c) Similar graphs as (a) except coated microtissues were treated with troglitazone. For drug toxicity data, statistical significance is relative to DMSO-treated control cultures. *p 0.05, ***p 0.001, and ****p 0.0001.

microenvironment that displayed higher PHH functions than conventional self-assembled spheroids and bulk hydrogels (herein referred to as "macrogels"); hepatic functions were enhanced and stabilized for 6+ weeks in the presence of supportive fibroblasts, although 3T3-J2 fibroblasts induced higher functions in PHHs than primary human HSCs. Placement of the microtissues into agarose microwells cast within multiwell plates prevented the aggregation of the microtissues and allowed probing with prototypical drugs for CYP induction and hepatotoxicity assays.

Human liver microtissues were compared to self-assembled spheroids and macrogels that are routinely used

to access 3D liver biology for structure–function studies and drug testing. All culture models enabled PHH functions for 2 weeks, confirming that a 3D microenvironment can sustain PHH functions over rapidly declining 2D monocultures on collagen I adsorbed onto plastic dishes[5,13]. However, the microtissues displayed significantly higher albumin and CYP450 enzyme activities than spheroids and macrogels. CYP450 enzymes metabolize >50% of marketed drugs, and their expression is influenced by age, sex, genetic polymorphisms, drugs/chemicals, hormones/cytokines, and disease states[30]. Thus, it is critical to maintain physiologically relevant levels of these enzymes in vitro toward elucidating in

vivo-like compound metabolism and toxicity[5,13]; our results suggest that microtissues may enable such an outcome over the conventional spheroids and macrogels.

The higher CYP450 activities in microtissues than spheroids and macrogels may be due to a more optimal and consistent microenvironment around PHHs. First, microtissues allow for the ligation of PHH integrins to the collagen immediately as opposed to the time-dependent ligation with cell-secreted ECM in the spheroids. Second, microtissues maintain a consistent inter- and intradonor ECM microenvironment as opposed to the likely variable ECM secretion rates by different donors in spheroids. Third, the microscale dimensions of microtissues likely facilitate the optimal delivery of oxygen and nutrients than the macrogels. Lastly, homotypic cell–cell interactions, which have been shown to be critical for PHH functions and polarity[5], are likely better facilitated within the microtissues than the macrogels at similar cell seeding densities. Therefore, microtissues may provide a more reproducible platform for drug development than conventional spheroids and macrogels.

In addition to generating higher liver-specific function, microtissues may also improve the logistical considerations for screening compounds over spheroids and macrogels. While microtissues were found to form robustly here with multiple PHH donors, spheroids are difficult to stably form with >50% of PHH donors[10], which may be due to differential ECM secretion rates across PHH donors. Furthermore, microtissues use ~10% of PHHs used in spheroids but still enable the highest CYP450 activities when normalized to cell numbers. Lastly, the fabrication of macrogels requires large amounts of expensive ECM and thus places considerable limits on the sample size for each condition; in contrast, hundreds of microtissues can be tracked for each condition. Therefore, PHH microtissues may allow the screening of large compound libraries or various disease stimuli with multiple PHH lots toward identifying lead molecules/pathways for further testing, either in vitro or in vivo.

Coculture with liver- and non-liver-derived NPC types can affect hepatocyte functions in the developing and adult livers[5,13]. Some of these interactions can be replicated in vitro by coculturing primary hepatocytes with NPCs, such as rat hepatocytes cocultured with either C3H/10T1/2 mouse embryo cells[31], 3T3-J2 murine embryonic fibroblasts[32], or human fibroblasts[33]. Of these, 3T3-J2 fibroblasts express molecules present in the liver [e.g., decorin, vascular endothelial growth factor (VEGF), and T-cadherin] at higher levels than other 3T3 fibroblast clones[34], which allows 3T3-J2 fibroblasts to induce higher PHH functions in 2D cocultures[7]. Furthermore, 3T3-J2 fibroblasts can induce higher levels of functions in PHHs than human liver sinusoidal endothelial cells[22], HSCs[23], and Kupffer cells[35], albeit in 2D culture formats.

Owing to the positive effects of 3T3-J2 fibroblasts on PHH functions, these fibroblasts were cocultured with PHHs in the microtissues via coencapsulation of both cell types or by coating the PHH-encapsulated collagen-based microtissues with fibroblasts; similarly, conventional self-assembled PHH spheroids and PHH-containing collagen macrogels were also coated with fibroblasts to elucidate the role of microscale collagen presentation on PHH functions in the presence of fibroblasts. The fibroblasts enhanced PHH functions over PHH monocultures placed within 3D microtissues, spheroids, and macrogels. However, the fibroblast-coated microtissues displayed significantly higher functions than both the coencapsulated microtissues, coated spheroids, and coated macrogels. The higher functions of the coated versus coencapsulated microtissues may be due to increased PHH homotypic contacts during compaction, which is crucial for PHH polarity and function, whereas coencapsulated microtissues only enable a randomly dispersed coculture that has been shown to be insufficient for promoting adequate PHH contacts even in 2D monolayers[7]. Additionally, coated microtissues were more homogenous in size after compaction as compared to coencapsulated microtissues, which may further enable consistent PHH homotypic contacts and, thus, higher function. On the other hand, while considerable compaction was also observed in the coated spheroids, the collagen scaffolding within the microtissues was necessary to further enhance PHH functions, suggesting that the increase in ECM density in the coated microtissues may also play a role in increased function. Finally, close interactions between 3T3-J2 fibroblasts and PHHs in microtissues (i.e., coated configuration) were necessary to enable the highest levels of hepatic functions as compared to paracrine-only interactions between PHH-only microtissues and 3T3-J2 fibroblasts seeded into Transwell inserts.

Primary HSCs, especially those that have been differentiated into myofibroblasts, have been previously shown to support some hepatic functions in vitro[23,36] even though they are implicated in causing liver fibrosis due to excessive collagen deposition in vivo[37]. Here we compared the effects of 3T3-J2 fibroblasts and primary human HSCs in induction of PHH functions within the 3D microtissues. HSC-coated microtissues displayed higher albumin secretion, CYP3A4 activity, and CYP2C9 activity than PHH-only microtissues, whereas CYP2A6 and CYP1A2 activities were similar across the two models. However, 3T3-J2-coated microtissues functionally outperformed HSC-coated microtissues for albumin secretion and three out of the four CYP enzyme activities measured (CYP3A4, CYP2A6, and CYP1A2), while CYP2C9 activity was similar in both models. Importantly, the expression of several critical liver genes relevant to drug disposition (*CYP2C8*, *CYP2C19*, *MRP2*, *SLCO1B1*, *and PXR*) was

undetectable after 6 weeks in HSC-coated microtissues but still detectable in the 3T3-J2-coated microtissues. These results suggest that the 3T3-J2-coated microtissues may be most suitable for routine assessment of drug responses in highly functional PHHs. Nonetheless, the ability of the HSC-coated microtissues to support PHH phenotype for several weeks in vitro suggests that the microtissue platform may be suitable to model PHH–HSC interactions in physiology and disease (e.g., excessive HSC proliferation and ECM deposition/reorganization induced via drugs and/or excess nutritional stimuli as in vivo).

In the 3T3-J2-coated microtissues, PHHs displayed long-term and relatively stable phenotype for 6+ weeks at comparable levels to freshly thawed PHHs with some noted exceptions. The expression levels of 13 of the 18 liver-specific genes measured were higher, while the levels of 5 of the 18 genes were downregulated to 55%–85% after 6 weeks in culture in the coated microtissues as compared to the levels in freshly thawed PHHs; nonetheless, all genes had detectable expression levels in coated microtissues over the entire culture duration. At the functional level, CYP2A6 and CYP1A2 activities in the coated microtissues recovered to within twofold of the levels in freshly thawed PHHs. On the other hand, albumin and urea secretions were not detected in freshly thawed PHHs but reached stable steady-state levels in coated microtissues, which may be due to the rapid degradation of secretory capacities following isolation of PHHs from the liver; indeed, recovery of albumin and urea secretions has also been observed previously in PHH/NPC cocultures[7,20,38]. Additionally, CYP3A4 and CYP2C9 activities in the coated microtissues were ~25%–30% of the activities measured in freshly thawed PHHs. Since CYP3A4 and 2C9 enzyme activities can be induced by several drugs[39,40], the initial presence of any inducer drugs in the donor's liver and thus PHHs may be a confounding factor in our findings. Nonetheless, the enhanced longevity of coated microtissues can potentially enable the elucidation of the chronic effects of drugs, industrial chemicals, and disease stimuli (e.g., hepatitis B virus, alcohol, and excess dietary triggers) on PHH functions.

The 3T3-J2-coated microtissues were found to display clinically relevant drug responses. Specifically, omperazaole induced CYP1A2 activity in microtissues, likely due to binding to aryl hydrocarbon receptor[41]; rifampin induced both CYP3A4 and CYP2C9, likely due to binding to pregnane X receptor[42]. Fold changes of CYP3A4 and CYP2C9 induction in coated microtissues were found to be higher than routinely utilized 2D PHH monocultures (~7-fold CYP3A4 induction and 5-fold CYP2C9 induction in coated microtissues versus 5.5-fold CYP3A4 induction and 1.4-fold CYP2C9 induction in 2D PHH monocultures); however, CYP1A2 induction was ~2-fold

lower in microtissues compared to 2D monocultures, likely due to the reduced expression of *AHR* in microtissues relative to freshly thawed PHHs. Regardless, proper enzyme responsiveness to known drugs, even after several weeks in culture, suggests that the microtissue platform is suitable for drug-mediated CYP induction assays.

In addition to CYP induction, coated microtissues were treated with troglitazone (hepatotoxin) or rosiglitazone (nonhepatotoxin) for 8 days and at concentrations up to $60\times C_{max}$ for each drug since these parameters were previously shown to allow appropriate appraisal of safety margins for diverse pharmaceuticals without causing an increase in the detection of false positives (i.e., loss of specificity)[21,25]. Rosiglitazone did not affect either PHH albumin or viability in the coated microtissues, which is consistent with its relatively safe profile with respect to liver liabilities in humans[29]. In contrast, troglitazone caused a time- and concentration-dependent loss of albumin secretion and cell viability. Coculture viability was affected more severely than albumin in the supernatants, which may be due to the detection of albumin from lysed PHHs; however, fibroblast contribution to the coculture viability trends requires further investigation using cell-specific staining markers. Furthermore, an appraisal of the overall sensitivity and specificity of microtissues for preclinical assessment of drug-induced hepatotoxicity would necessitate testing of a larger panel of drugs (>50) from diverse classes and mechanisms of action, which we plan to pursue in follow-up studies. Nonetheless, the proof-of-concept data here suggest that 3T3-J2 fibroblast coating does not inhibit the utility of microtissues for investigating PHH responses to compounds following repeat exposure.

Our modular microtissues can be further tuned to investigate other features of the PHH microenvironment in the liver. First, collagen I can be augmented with additional liver-inspired ECM molecules such as other collagens (e.g., collagen IV), fibronectin, laminin, and proteoglycans (e.g., decorin). Second, custom microtissues containing liver NPCs, such as liver sinusoidal endothelial cells, HSCs, and Kupffer cells, can be created to test specific hypotheses around PHH–NPC interactions in physiology and disease. Lastly, microfluidic devices can be used to induce gradients of oxygen and hormones across microtissues to mimic differential PHH functions as in liver zonation[43], which can be useful to determine whether identified toxic compounds show a zonal preference[44].

In conclusion, we showed that 3D collagen I microtissues containing PHHs display phenotypic stability, including CYP450 enzyme activities, for at least 6 weeks within multiwell plates without the need for any fluid perfusion. PHH functions in such microtissues can be further

enhanced via coated coculture with primary human HSCs or 3T3-J2 fibroblasts, with the latter providing for the highest levels for the majority of PHH functions. Finally, we showed that 3T3-J2-coated 3D microtissues are suitable to assess drug-mediated CYP induction and hepatotoxicity following repeat drug exposure. Ultimately, the functionally optimized microtissues could serve to reduce drug attrition, enable the screening of molecules to optimize cell functions in cell-based therapies, and aid in the studies of liver physiology and disease.

REFERENCES

1. Underhill GH, Khetani SR. Bioengineered liver models for drug testing and cell differentiation studies. Cell Mol Gastroenterol Hepatol. 2018;5(3):426–39 e1.

2. Lin C, Ballinger KR, Khetani SR. The application of engineered liver tissues for novel drug discovery. Expert Opin Drug Discov. 2015;10(5):519–40.

3. Bhatia SN, Underhill GH, Zaret KS, Fox IJ. Cell and tissue engineering for liver disease. Sci Transl Med. 2014;6(245):245sr2.

4. Schwartz RE, Fleming HE, Khetani SR, Bhatia SN. Pluripotent stem cell-derived hepatocyte-like cells. Biotechnol. Adv. 2014;32(2):504–13.

5. Godoy P, Hewitt NJ, Albrecht U, Andersen ME, Ansari N, Bhattacharya S, Bode JG, Bolleyn J, Borner C, Böttger J, et al. Recent advances in 2D and 3D in vitro systems using primary hepatocytes, alternative hepatocyte sources and non-parenchymal liver cells and their use in investigating mechanisms of hepatotoxicity, cell signaling, and ADME. Arch Toxicol. 2013;87(8):1315–530.

6. Stevens KR, Scull MA, Ramanan V, Fortin CL, Chaturvedi RR, Knouse KA, Xiao JW, Fung C, Mirabella T, Chen AX, et al. In situ expansion of engineered human liver tissue in a mouse model of chronic liver disease. Sci Transl. Med. 2017;9(399).

7. Khetani SR, Bhatia SN. Microscale culture of human liver cells for drug development. Nat Biotechnol. 2008;26(1):120–26.

8. Foster AJ, Chouhan B, Regan SL, Rollison H, Amberntsson S, Andersson LC, Srivastava A, Darnell M, Cairns J, Lazic SE, et al. Integrated in vitro models for hepatic safety and metabolism: Evaluation of a human liver-chip and liver spheroid. Arch Toxicol. 2019;93:1021–37.

9. Li X, George SM, Vernetti L, Gough AH, Taylor DL. A glass-based, continuously zonated and vascularized human liver acinus microphysiological system (vLAMPS) designed for experimental modeling of diseases and ADME/TOX. Lab Chip 2018;18(17):2614–31.

10. Bell CC, Hendriks DFG, Moro SML, Ellis E, Walsh J, Renblom A, Fredriksson Puigvert L, Dankers ACA, Jacobs F, Snoeys J, et al. Characterization of primary human hepatocyte spheroids as a model system for drug-induced liver injury, liver function and disease. Sci Rep. 2016;6:25187.

11. Messner S, Agarkova I, Moritz W, Kelm JM. Multi-cell type human liver microtissues for hepatotoxicity testing. Arch Toxicol. 2013;87(1):209–13.

12. Norona LM, Nguyen DG, Gerber DA, Presnell SC, LeCluyse EL. Editor's highlight: Modeling compound-induced fibrogenesis in vitro using three-dimensional bioprinted human liver tissues. Toxicol. Sci. 2016;154(2):354–67.

13. Khetani SR, Berger DR, Ballinger KR, Davidson MD, Lin C, Ware BR. Microengineered liver tissues for drug testing. J Lab Autom. 2015;20(3):216–50.

14. Corstorphine L, Sefton MV. Effectiveness factor and diffusion limitations in collagen gel modules containing HepG2 cells. J Tissue Eng Regen Med. 2011;5(2):119–29.

15. Brett M-E, Crampton AL, Wood DK. Rapid generation of collagen-based microtissues to study cell–matrix interactions. Technology 2016;04(02):80–7.

16. Cummins KA, Crampton AL, Wood DK. A high-throughput workflow to study remodeling of ecm-based microtissues. Tissue Eng Part C Methods 2019;25(1):25–36.

17. Chen Q, Utech S, Chen D, Prodanovic R, Lin JM, Weitz DA. Controlled assembly of heterotypic cells in a core–shell scaffold: Organ in a droplet. Lab Chip 2016;16(8):1346–9.

18. Siltanen C, Diakatou M, Lowen J, Haque A, Rahimian A, Stybayeva G, Revzin A. One step fabrication of hydrogel microcapsules with hollow core for assembly and cultivation of hepatocyte spheroids. Acta Biomater. 2017;50:428–36.

19. Li CY, Stevens KR, Schwartz RE, Alejandro BS, Huang JH, Bhatia SN. Micropatterned cell–cell interactions enable functional encapsulation of primary hepatocytes in hydrogel microtissues. Tissue Eng. Part A 2014;20(15–16):2200–12.

20. Schepers A, Li C, Chhabra A, Seney BT, Bhatia S. Engineering a perfusable 3D human liver platform from iPS cells. Lab Chip 2016;16(14):2644–53.

21. Khetani SR, Kanchagar C, Ukairo O, Krzyzewski S, Moore A, Shi J, Aoyama S, Aleo M, Will Y. Use of micropatterned cocultures to detect compounds that cause drug-induced liver injury in humans. Toxicol Sci. 2013;132(1):107–17.

22. Ware BR, Durham MJ, Monckton CP, Khetani SR. A cell culture platform to maintain long-term phenotype of primary human hepatocytes and endothelial cells. Cell Mol Gastroenterol Hepatol. 2018;5(3):187–207.

23. Davidson MD, Kukla DA, Khetani SR. Microengineered cultures containing human hepatic stellate cells and hepatocytes for drug development. Integr Biol. 2017; 9(8):662–77.

24. Berger DR, Ware BR, Davidson MD, Allsup SR, Khetani SR. Enhancing the functional maturity of induced pluripotent stem cell-derived human hepatocytes by controlled presentation of cell–cell interactions in vitro. Hepatology 2015;61(4):1370–381.

25. Xu JJ, Henstock PV, Dunn MC, Smith AR, Chabot JR, de Graaf D. Cellular imaging predictions of clinical drug-induced liver injury. Toxicol Sci. 2008;105(1):97–105.

26. Collins TJ. ImageJ for microscopy. BioTechniques 2007;43(1 Suppl):25–30.

27. Pluen A, Netti PA, Jain RK, Berk DA. Diffusion of macromolecules in agarose gels: Comparison of linear and globular configurations. Biophys J. 1999;77(1):542–52.

28. Fatin-Rouge N, Starchev K, Buffle J. Size effects on diffusion processes within agarose gels. Biophys J. 2004;86(5):2710–9.

29. Isley WL. Hepatotoxicity of thiazolidinediones. Expert Opin Drug Saf. 2003;2(6):581–6.

30. Zanger UM, Schwab M. Cytochrome P450 enzymes in drug metabolism: Regulation of gene expression, enzyme activities, and impact of genetic variation. Pharmacol Ther. 2013;138(1):103–41.

31. Langenbach R, Malick L, Tompa A, Kuszynski C, Freed H, Huberman E. Maintenance of adult rat hepatocytes on C3H/10T1/2 cells. Cancer Res. 1979;39(9):3509–14.

32. Bhatia SN, Balis UJ, Yarmush ML, Toner M. Effect of cell–cell interactions in preservation of cellular phenotype: Cocultivation of hepatocytes and nonparenchymal cells. FASEB J. 1999;13(14):1883–900.

33. Michalopoulos G, Russell F, Biles C. Primary cultures of hepatocytes on human fibroblasts. In Vitro 1979;15(10):796–806.

34. Khetani SR, Szulgit G, Del Rio JA, Barlow C, Bhatia SN. Exploring interactions between rat hepatocytes and nonparenchymal cells using gene expression profiling. Hepatology 2004;40(3):545–54.

35. Nguyen TV, Ukairo O, Khetani SR, McVay M, Kanchagar C, Seghezzi W, Ayanoglu G, Irrechukwu O, Evers R. Establishment of a hepatocyte–Kupffer cell coculture model for assessment of proinflammatory cytokine effects on metabolizing enzymes and drug transporters. Drug Metab Dispos. 2015;43(5):774–85.

36. Abu-Absi SF, Hansen LK, Hu W-S. Three-dimensional coculture of hepatocytes and stellate cells. Cytotechnology 2004;45(3):125–40.

37. Friedman SL. Hepatic stellate cells: Protean, multifunctional, and enigmatic cells of the liver. Physiol Rev. 2008;88(1):125–72.

38. Vernetti LA, Senutovitch N, Boltz R, Debiasio R, Shun TY, Gough A, Taylor DL. A human liver microphysiology platform for investigating physiology, drug safety, and disease models. Exp Biol Med. 2016;241(1):101–14.

39. Lin C, Shi J, Moore A, Khetani SR. Prediction of drug clearance and drug–drug interactions in microscale cultures of human hepatocytes. Drug Metab Dispos. 2016;44(1):127–36.

40. Hewitt NJ, de Kanter R, LeCluyse E. Induction of drug metabolizing enzymes: A survey of in vitro methodologies and interpretations used in the pharmaceutical industry—Do they comply with FDA recommendations? Chem Biol Interact. 2007;168(1):51–65.

41. Diaz D, Fabre I, Daujat M, Saint Aubert B, Bories P, Michel H, Maurel P. Omeprazole is an aryl hydrocarbon-like inducer of human hepatic cytochrome P450. Gastroenterology 1990;99(3):737–47.

42. LeCluyse EL. Pregnane X receptor: Molecular basis for species differences in CYP3A induction by xenobiotics. Chem Biol Interact. 2001;134(3):283–89.

43. Bahar Halpern K, Shenhav R, Matcovitch-Natan O, Toth B, Lemze D, Golan M, Massasa EE, Baydatch S, Landen S, Moor AE, et al. Single-cell spatial reconstruction reveals global division of labour in the mammalian liver. Nature 2017;542(7641):352–6.

44. Anundi I, Lähteenmäki T, Rundgren M, Moldeus P, Lindros KO. Zonation of acetaminophen metabolism and cytochrome P450 2E1-mediated toxicity studied in isolated periportal and perivenous hepatocytes. Biochem. Pharmacol. 1993;45(6):1251–9.